Colloid Polym Sci 273:1193–1200 (1995)

ORIGINAL CONTRIBUTION

H. Hirata
H. Okabayashi
M. Furusaka
T. Kawakatsu

A small angle neutron scattering study of the sodium di-*n*-pentyl phosphate micelles in water

Received: 20 April 1995
Accepted: 26 July 1995

H. Hirata · Dr. H. Okabayashi (✉)
Department of Applied Chemistry
Nagoya Institute of Technology
Gokiso-cho, Showa-ku
Nagoya 466, Japan

M. Furusaka
BSF, National Laboratory for
High Energy Physics
1-1 Oho, Tsukuba-shi
Ibaraki 305, Japan

T. Kawakatsu
Department of Physics
Tokyo Metropolitan University
Hachioji
Tokyo 192-03, Japan

Abstract Small angle neutron scattering has been used to elucidate the size and shape of a micelle in the sodium di-*n*-pentyl phosphate (DPP)-water system. The results are summarized as follows. For the DPP micelle, the aggregation number (**n**) depends on the concentration (**n** = 12, at 7.0 wt% and **n** = 15 at 10.0 wt%). The minimum micelle is spherical and has an aggregation number **n** = 7. For the DPP-micellar system, it can be assumed that micellar growth and variation from the spherical to prolate shape occurs with an increase in concentration above the CMC.

Key words Sodium di-*n*-pentyl-phosphate – micelle – SANS

Introduction

Much attention has been given to structural studies of dialkylphosphates having two long *n*-alkyl chains in an aggregated state [1–11]. Synthesized amphiphiles, such as didecyl, didodecyl and dihexadecyl phosphates, have been shown to form vesicles and lamellar structures that possess physicochemical characteristics similar to those of biomembranes [2, 3].

When such an organized structure of surfactant molecules is formed in aqueous solution, conformational change of a hydrocarbon chain and environmental variation of the hydrated polar groups should occur. The structural change at the interface may be associated with the functional appearance of a biomembrane. However, such detailed studies have been very few although they are highly desirable. For dialkylphosphate molecules having long *n*-alkylchains, both the solubility and the critical micelle concentration (CMC) in aqueous solution are very low. These properties prevent making a detailed study of any conformational change of surfactant molecules occurring below and above the CMC. However, for simple dialkylphosphate molecules both the solubility and the CMC in aqueous solutions are very high. Therefore, we may then make a direct investigation of the conformational change of the surfactant molecules and of the structural variation at the micellar interface which are a consequence of micellization.

Conformational studies on dialkylphosphates in the aggregated state are important for understanding the aggregation structure of phospholipid bilayers. Thus far, the conformation of simple dialkylphosphate anions in aqueous solution has been mainly investigated by infrared and Raman spectroscopic methods [12–14]. Raman studies of dibutylphosphate anions [14] have provided direct evidence that micelle formation of the dialkylphosphate anions brings about an increase in population of the all-*trans*

hydrocarbon. Similar observations have already been reported for aqueous solutions of simple soap molecules. For potassium *n*-butnanote, *n*-pentanoate and *n*-hexanoate in the solid state and in aqueous solution, Raman scattering spectra have also been measured, and the concentration dependence of the molecular conformations of these molecules has been investigated in detail by the use of the accordion vibrations derived from the all-*trans* hydrocarbon chains [15, 16]. The results have indicated that the percentage of the all-*trans* hydrocarbon chains increases with an increase in concentration above the CMC. Such a conformational change, seen when simple surfactants undergo micellization, must be closely associated with the structure of aggregates.

In this study, we report the detailed micellar structure in the binary di-*n*-pentyl phosphate-water system determined by analysis of small angle neutron scattering spectra. In particular, the micellar structure is discussed in connection with the molecular conformation of the di-*n*-pentyl phosphate anion.

Experimental

Material

Sodium di-*n*-pentyl phosphate (DPP) was prepared as follows. *n*-Pentylphosphorodichloridate (*n*-pentyl-OP(O)Cl_2, b.p 75 ~77 °C at 4 mmHg), prepared using phosphoryl chloride and *n*-pentyl alcohol and vacuum-distilled, was converted to di-*n*-pentylphosphorochloridate ((*n*-pentyl-O)$_2$P(O)Cl) [17]. The (*n*-pentyl-O)$_2$P(O)Cl sample was vacuum-distilled several times (b.p. 108 ~110 °C at 4 mmHg) and was treated with benzaldoxim (Furuka Chemie AG) by the method of Mukaiyama et al. [18], to yield phosphoric acid di-*n*-pentyl ester, (*n*-pentyl-O)$_2$P(O)OH. The ester was neutralized with a solution of NaOH, and the sodium salt was recrystallized in aqueous acetone. The identification of DPP was made by ^{1}H and ^{13}C NMR spectral analysis. Since the Na salt was hygroscopic, the Ba salt was used for the elemental analysis. Anal. $C_{20}H_{44}O_8P_2Ba$: Calcd: C, 39.26; H, 7.25. Found: C, 39.06; H, 7.47.

Molal volume determinations

The apparent molal volumes (Φ_{app}) of a di-*n*-pentyl phosphate anion were calculated from the densities of the sample-H_2O solutions. The density of the sample solution was measured with a Lipkin–Davison type pycnometer calibrated with the known density of water. The temperature of the thermostated-bath system was controlled at 298.00 ± 0.02 K.

Table 1 Volumes (V, Å^3) and Scattering lengths (Σb_{coh}, Å)

Species	V	Σb_{coh}
CH_3	42.6*	-0.457×10^{-4}
CH_2	28.2*	-0.083×10^{-4}
PO_4^-	50.8	2.845×10^{-4}
Na^+	3.6**	0.363×10^{-4}
D_2O	30.2**	1.918×10^{-4}
H_2O	29.9**	-0.165×10^{-4}

* ref. 19 ** ref. 20

Neutron scattering measurements

The SANS measurements were carried out using a small and medium angle neutron scattering instrument (WINK) installed at the pulsed neutron source KENS at the National Laboratory for High Energy Physics, Tsukuba, Japan. The sample solutions were placed in a quartz cell of 2 mm path length. The scattering length density (ρ) of each component was calculated using Eq. (1),

$$\rho = \Sigma b_i / V \tag{1}$$

where b_i is the scattering length of atom i and V is the molecular volume. The scattering length densities used for the SANS data analysis are listed in Table 1. The magnitude of the momentum transfer (Q) is given by Eq. (2),

$$Q = \frac{4\pi}{\lambda} \sin\left(\frac{\theta}{2}\right) \tag{2}$$

where λ is the incident wavelength (1 ~16 Å) and θ the scattering angle. The intensity scattered by neutrons was recorded on a position-sensitive 2-D detector. Normalization of the data to an absolute intensity scale was made by using the transmission of a 1 mm water sample. Corrections for the attenuation of the beam due to absorption and for multiple scattering were also made [21].

Results and discussion

Partial molar volume of the DPP anion

The density of the DPP anions against concentration (Fig. 1[A]) provides two straight lines whose intersection gives the same value for the CMC as obtained from measurements of the self-diffusion coefficient [22]. From these density data, we can calculate the partial molar volume of the DPP anion in the monomeric and micellar

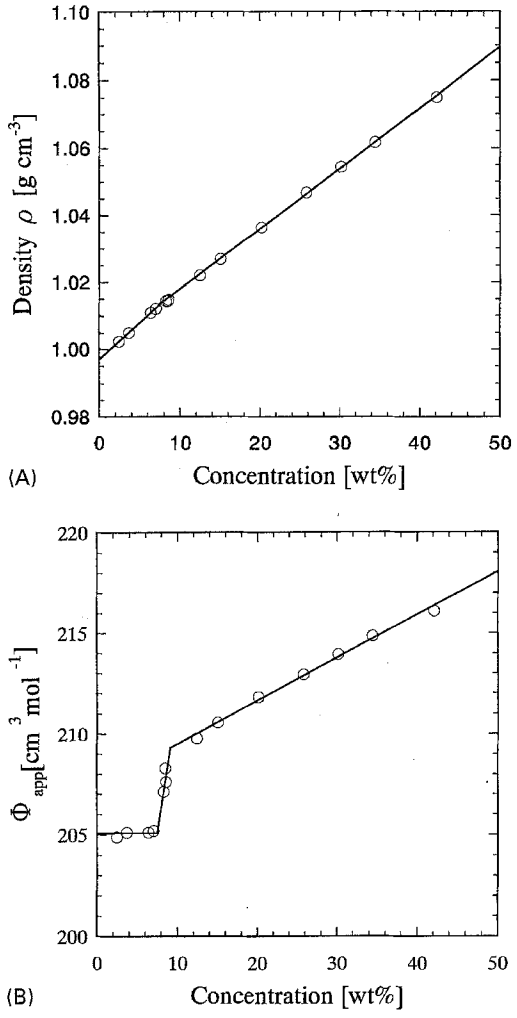

Fig. 1 Concentration dependence of the density (ρ) ([A]) and Φ_{app} value ([B]) at 25.00 ± 0.02 °C

states. The apparent molar volume Φ_{app} is calculated from the density (d) of the solution expressed in g cm^{-3} using Eq. (3),

$$\Phi_{app} = \frac{1}{m}\left[\frac{1000 - mM}{d} - \frac{1000}{d_s}\right] \tag{3}$$

where m is the molarity, ρ_s the density of the solvent and M the molar weight of the solute. The partial molar volume (Φ) of the solute can be obtained from Eq. (4).

$$\Phi = \Phi_{app} - 1.868C^{1/2}. \tag{4}$$

In the plots of Φ_{app} vs. C, as shown in Fig. 1 [B], the Φ values are almost constant at concentrations below 7.4 wt%. However, after a rapid increase at 7.4 wt% they increase linearly with an increase in concentration. The concentration at 7.4 wt% can be regarded as the CMC. This value is larger than those (4.6 ~4.7 wt%) determined from plots of ln D vs. $1/C$ and ^{31}P σ vs. $1/C$ [22]. However, since H_2O is used as solvent for the density measurements, it might be expected that the CMC value should be smaller by factor of a 10%, as observed. Above the CMC the Φ value is expressed by Eq. (5),

$$\Phi = \frac{\mathrm{CMC}}{C}\Phi_0 + \frac{C - \mathrm{CMC}}{C}\Phi_a \tag{5}$$

where Φ_a denotes the partial molar volume of the micellar DPP anion.

The Φ_0 and Φ_a values obtained for the DPP anions are 204.4 and 220.0 cm^3 mol^{-1}, respectively, and are used for the SANS data analysis.

SANS spectra and micellar structure

The dependence of neutron scattered intensity on the magnitude of a scattering vector (Q) depends upon both the particle structure factor $P(Q)$ and the interparticle structure factor $S'(Q)$. $S'(Q)$ is a function of the diameter (σ), charge (Z) and number density of a particle and of the dielectric constant of the solvent.

For a monodispersed system of charged hard particles, the scattering intensity can be expressed [23] as the product of $S'(Q)$ and $P(Q)$ in the following form,

$$\frac{d\Sigma(Q)}{d\Omega} = n_p 10^{-16}[(\rho_p - \rho_c)V_c + (\rho_s - \rho_p)V_m]^2 P(Q)S'(Q) \tag{6}$$

$$n_p = \frac{(C - \mathrm{CMC})N_A}{1000\mathbf{n}}[\mathrm{cm}^{-1}] \tag{7}$$

where n_p denotes the number density of the particles, and $\mathbf{n}$ the average aggregation number of a micelle, and

$$P(Q) = \int_0^1 |F(Q, \mu)|^2 \, d\mu \tag{8}$$

$$F(Q, \mu) = x\left(\frac{3(\sin(R_1) - R_1\cos(R_1))}{R_1^3}\right) + (1 - x)\left(\frac{3(\sin(R_2) - R_2\cos(R_2))}{R_2^3}\right) \tag{9}$$

$$x = \frac{(\rho_p - \rho_c)V_c}{(\rho_p - \rho_c)V_c + (\rho_s - \rho_p)V_m} \tag{10}$$

where V_c [Å^3] and V_m [Å^3] are the volumes of the micellar core and overall micelle, respectively. ρ_p [Å^{-2}], ρ_c [Å^{-2}] and ρ_s [Å^{-2}] are the average neutron scattering length density of the polar shell, hydrophobic core and solvent, respectively.

When the micellar shape is prolate, R_1, R_2 are given by

$$R_1 = [a^2\mu^2 + b^2(1 - \mu^2)]^{1/2} \quad (11)$$

$$R_2 = [(a + t)^2\mu^2 + (b + t)^2(1 - \mu^2)]^{1/2} \quad (12)$$

where **a** [Å] and **b** = 7.8 [Å] are diameters of the micellar axes [24] and **a** is a function of **n**, and **t** [Å] the diameter (4.6 [Å]) of the polar head group (PO_4^-).

The interparticle structure factor $S'(Q)$ can be calculated approximately by use of the following equation

$$S'(Q) = 1 + \beta(Q,\mu)[S(Q) - 1] \quad (13)$$

$$\beta(Q,\mu) = \frac{|\langle F(Q,\mu)\rangle^2|}{\langle |F(Q,\mu)|^2\rangle} \quad (14)$$

$$S(Q) = \frac{1}{[1 - 24\eta a(Q)]} \quad (15)$$

where η is the volume fraction of macroion and $a(Q)$ is given by Hayter and Penford [25, 26]. In this model, the micelle is assumed to be a rigid charged sphere of diameter σ [27, 28], interacting through a dimensionless screened Coulomb potential. The dimensionless screened Coulomb potential is calculated by using the inverse screening length of the Debye–Hückel theory, defined by the ionic strength I of the solution.

When the concentration of surfactant is very low and the intermicellar interaction is neglected, the intensity spectrum is dominated by $P(Q)$, and $S(Q)$ is unity throughout the observed Q range. However, when the interaction cannot be neglected as the concentration increases, $S(Q)$ deviates from unity and the interaction peak appears in the intensity spectrum.

For the micellar solution of DPP in water, the SANS experiment has been carried out at 23 ± 0.1 °C in the concentration range 6.0 ~10.0 wt%. It has been assumed that a DPP-micelle has a hydrophobic core with a major axis **a** and a minor axis **b** equal to those of the fully extended hydrocarbon chain length and that the polar head groups (diameter = **t**) associated with water molecules are soaked in bulk water. A structural model of the DPP micelle is inserted in Fig. 2.

In the present study, both prolate and oblate spheroid models for DPP micelles have been calculated by assuming mono- and poly-dispersity. We have found that the prolate spheroid model provides consistently better fits to the observed SANS data than does the oblate spheroid model. The results analyzed on the basis of mono-dispersity are summarized in Table 2(a). In the SANS analysis, the intensity spectrum of a DPP solution measured at concentrations below the CMC was subtracted from the intensity spectra of the solutions containing micelles in the Q range 0.06 ~0.60. The intensity spectra obtained for the DPP micellar solutions are shown in Fig. 2. The scattered intensities ($I(Q)$) observed in this concentration region are weak, because of low molecular weights. However, the experimental uncertainty of the results is of the order of ± 2%. In the curve of $I(Q)$ against Q obtained in the concentration range 7.0 ~10.0 wt%, very broad peaks are observed, showing that there are interactions between the micelles. As the concentration is changed from 7.0 wt% to 10.0 wt%, the interaction peak increases steadily and shifts slightly to higher Q values, indicating an enhanced interparticle structure factor with increasing micellar concentration. The closeness of fit between the observed data points and the theoretically calculated results is excellent (Fig. 2) and the average percentage deviation per data point was ± 5% for all spectra. The parameters (**n** and α) of fit are also listed in Table 2(a).

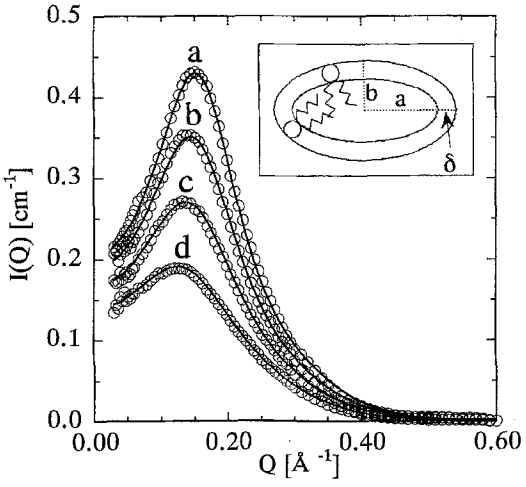

Fig. 2 Observed scattering intensity spectra (open circles) for the DPP-D_2O system at 23 °C: a 10 wt%, b 9 wt%, c 8 wt% and d 7 wt%, and fitted scattering intensity profiles (solid lines) in the Q range 0.06 ~0.60 [Å^{-1}], assuming that the micelles are monodispersed. The schematic model of the DPP micelle is inserted

The aggregation number of a DPP micelle is shown in Fig. 3 as a function of the square root of the monomer concentration (molar fraction) attributable to formation of micelles. We may assume that the aggregation number (**n**) tends to become small with a decrease in concentration (**n** = 12 at 7.0 wt% and **n** = 15 at 10.0 wt%). Moreover, all the **n** values fall on a straight line. Therefore, a ladder model of micellar growth can be applied to the micellar formation of DPP anions [29]. Furthermore, as can be seen in Table 2(a), the shape of a DPP micelle is prolate and the **a**/**b** ratio has a tendency to decrease as the concentration approaches the CMC. Therefore, we may assume that the micellar shape changes at concentrations above the CMC. The SANS spectra of sample solutions at concentrations near the CMC will be very weak in intensity, making it very difficult to obtain the particle structure

Table 2 The results of SANS data analysis

C[wt%]	7.0	8.0	9.0	10.0
(a) mono-dispersed				
n	12.4	13.1	14.0	14.8
a/b	1.92	2.03	2.17	2.29
α	0.48	0.46	0.43	0.30
N_S	21.3	20.9	20.5	20.1
σ[Å]	28.7	29.1	29.7	30.1
κ[Å]	6.46	6.33	6.23	6.16
η	0.063	0.089	0.113	0.138
(b) poly-dispersed				
$\mathbf{n}_{ave}$	13	14	15	16
$\mathbf{n}_{min}$	6	7	7	8
$\mathbf{n}_{max}$	20	21	23	24
α	0.50	0.49	0.45	0.32

n: The average aggregation number of a micelle
a/b: Micellar axis ratio **b** = 7.8 [Å]
α: The degree of ionization of a micelle
N_S: The number of water molecules associated with a PO_4^- group
σ: The macro-ion diameter
κ: The inverse screening length of Debye-Hückel theory
η: Volume fraction of macro-ion

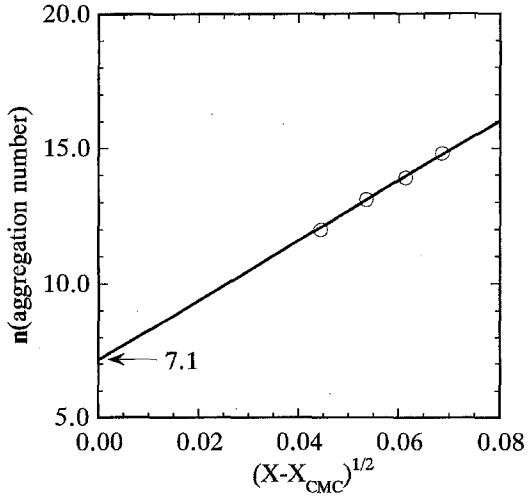

Fig. 3 A plot of **n** as a function of the square root of monomer concentration-forming-micelles

factor of the just-born micelle. However, we can assume a minimum aggregation number (**n** = 7) for a micelle at the CMC by extrapolation of the linear $(X\text{-}X_{CMC})^{1/2}$ vs **n** plots, as shown in Fig. 3. Under these conditions, an **a/b** ratio of 1.1 can be calculated, showing that the minimum micelle is spherical. Thus, for the micellar system of DPP anions it can be assumed that micellar growth and variation from the spherical to the prolate shape occurs with an increase in concentration above the CMC. The rationale for proposing a minimum micelle of aggregation number **n** = 7 can be seen from the following geometrical consideration.

The hydrocarbon core volume of a DPP micelle having an aggregation number **n** = 7 is 2173 Å^3, since the volume of the two *n*-pentyl chains of a DPP molecule is 311 Å^3. If we assume that the shape of a DPP micelle is spherical and that the radius of the micellar core is equal to the length (7.8 Å) of a pentyl chain taking up the all-*trans* form, (given by Tanford's equation [24]), then the volume of the micelle will be 2010 Å^3, and we can calculate an aggregation number of 6.5, by dividing the volume of 2010 Å^3 by the volume (311 Å^3) of the two pentyl chains. This value is almost the same as the minimum aggregation number **n** = 7.

As has already been demonstrated directly in our preceding papers [15, 16], for the aqueous solutions of simple soap molecules (potassium *n*-pentanoate and *n*-hexanoate) and barium dibutyl and dipentylphosphate molecules, the percentages of rotational isomers containing the *gauche*-forms are relatively high below the CMC, compared with that of the all-*trans*-form. However, micellization brings about preferential stabilization of the all-*trans* hydrocarbons. These experimental results are consistent with a micellar model having the extended structure of hydrocarbon chains outlined above.

Micelles of the double-chain anionic surfactant AOT have been studied in aqueous solutions by Sheu et al. [30] by using SANS. They assumed that the minimum aggregation number at the CMC was 15 ± 1 and that the micellar shape was spherical. Furthermore, it was assumed that the AOT micelles grew as the concentration increased and were transformed from a spherical to an oblate spherical shape. For the micellar solutions of ammonium octanoate in aqueous solution [31], it has already been found from SANS that the aggregation number depends upon the concentration: **n** = 7 at 0.36 mol l^{-1} and **n** = 12 at 0.48 mol l^{-1}.

We have analyzed the scattering intensity curves taken from sample solutions of different H_2O–D_2O mixtures. The contrast variation method at finite Q used in the present study is based on a Q-dependent quantity $A(Q)$ given by Sheu et al. [28].

$$A(Q) = [(d\Sigma(Q)/d\Omega)/P(Q)/S'(Q)]^{1/2} \tag{16}$$

$A(Q)$ can be calculated from the observed SANS spectra combined with the model calculations of $P(Q)$ and $S'(Q)$. $\langle A(Q)\rangle$ is linearly proportional to the scattering length density of the $[D_2O]/[H_2O]$ mixed solvent. Therefore, the contrast matching point, where the scattering intensity vanishes, can be determined by extrapolating the $\langle A(Q)\rangle$ vs. ρ_s curve to zero.

Figure 4 shows the experimental and fitted curves of the scattering intensity vs Q plots for the DPP solution (10.0 wt%) at various $[D_2O]$:$[H_2O]$ ratios. The agreement is excellent across the whole range of samples. The

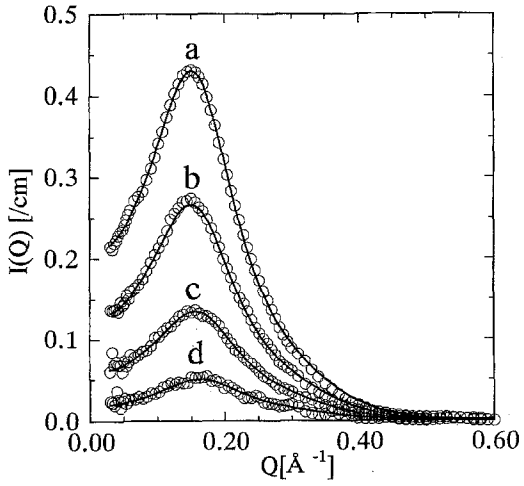

Fig. 4 Observed scattering intensity spectra (open circles) for the 10 wt% DPP solution at various D_2O% in the solvent: a 100% D_2O, b 80% D_2O, c 60% D_2O and d 40% D_2O, and fitted scattering intensity profiles (solid lines) in the Q range 0.06 ~0.60 [$Å^{-1}$], assuming that the micelles are mono-dispersed

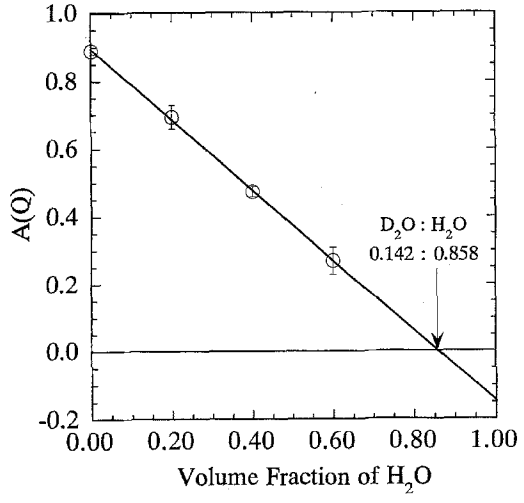

Fig. 5 External contrast variation plots for the 10 wt% DPP solution

used parameters (**n** and α) of fit and the extracted parameters are also listed in Table 2(a). Figure 5 shows the contrast variation ($A(Q)$ vs. ρ_s) plots. It is found by extrapolation that the contrast matching point occurs at a ratio of $[D_2O]:[H_2O] = 0.142:0.858$. The mean aggregation number (**n**) and volume value (V_{mol}) of a DPP molecule obtained from the slope and matching point are 14 and 348 $Å^3$, respectively.

In the micellar structure, which has a hydrophilic region containing the polar head group, counter ions and the water molecules of hydration, in addition to a hydrophobic region, Eq. (16) can be applied at the contrast matching point,

$$(\rho_c - \rho_p)V_c + (\rho_p - \rho_s)V_m = 0 \tag{17}$$

V_c and V_m denote the volume of the hydrophobic core and that of the whole micelle containing the polar layer, respectively, and ρ_c, ρ_p and ρ_s are the scattering length densities of the hydrophobic region, polar layer and solvent, respectively.

The contrast matching point has been calculated, taking into account the mean value ($\alpha = 0.30$) for the degree of ionization, and has been found to occur at a ratio of $[D_2O]:[H_2O] = 0.139:0.861$. The calculated and observed matching point values are almost identical.

The SANS analysis provides the degree (α) of ionization of a micelle (Table 2(a)), associated with the electric-double layer at the interface. As the concentration increases, the α value tends to decrease. It should be noted that the α value becomes very small (0.3) at a concentration of 10 wt%, which is very close to the second CMC (10.7 wt%) determined by the concentration dependence of the self-diffusion coefficient [22]. Accordingly, in the concentration region above the second CMC (17 wt%), determined by the ^{31}P NMR chemical shift [18], we may expect that the degree of ionization for the aggregate system will become extremely small compared with that at 10 wt%. For the DPP-water solution, it may be assumed from the results of the ^{31}P NMR and x-ray low angle diffraction patterns [22] that a highly-organized structure, similar to a lamellar structure, is formed at high concentrations. It is very difficult to estimate the degree of ionization at the lamellar interface by SANS analysis. However, we may speculate that most of the counter ions are condensed at the interface of a lamellar structure.

Usually, we may assume that micelles in equilibrium with each other in solution have a finite distribution of sizes about some mean value. In the present study, the scattering intensity ($d\Sigma(Q)/d\Omega$) was also calculated by considering the polydispersity and use was also made of the interparticle structure factor $S'(Q)$, (Eq. (13)).

For the size-dispersed system of charged hard particles, the scattering intensity can be expressed in the following form,

$$\frac{d\Sigma(Q)}{d\Omega} = \left(\sum_{i=i_{min}}^{i_{max}} n_p(i)[(\rho_p(i) - \rho_c(i))V_c(i) + (\rho_s(i) - \rho_p(i))V_m(i)]^2 P(i, Q) \right) S'(Q) \tag{18}$$

$$n_p = \frac{(C - CMC)d(i)N_A}{1000i} [cm^{-3}] \tag{19}$$

where (*i*) denotes the particles having aggregation number *i*, and *d*(*i*) is the concentration distribution function of the monomer. It is assumed that *d*(*i*) is a Gausian function with standard deviation (square root of mean average aggregation number) [32].

The calculated $d\Sigma(Q)/d\Omega$ profiles are not shown here. The average aggregation number ($\mathbf{n}_{ave}$), and the minimum and maximum values of the aggregation number are listed in Table 2(b). It can be seen that the $\mathbf{n}_{ave}$ values are very similar to the aggregation number calculated by assuming monodispersity.

Molecular Conformations in the DPP Micelle

For di-*n*-butyl or di-*n*-pentyl phosphate anions in water, we have already demonstrated that the all-trans form of the alkyl group is preferentially stabilized upon micellization [13, 14]. Therefore, in the SANS spectral analysis, the assumption that the radius of the micellar core is equal to the length of an extended pentyl chain is well supported by these experimental results.

Furthermore, for the conformations about the two PO–CC single bonds, it has been found that micellization brings about preferential stabilization of the trans form [33]. Accordingly, in the DPP micelle, we may assume that the pentyloxy segments are in an extremely restricted state.

However, in the DPP-micellar system, conformations about the two phosphodiester P–O bonds seem to play an important role. As shown in Fig. 6, for the DPP molecule only three molecular forms (GG, GT and TT) about the P–O bonds can be considered: four mirror images (G′G′, G′T, TG and TG′) can be omitted and the GG′ and G′G forms are also omitted because of their instability due to steric hindrance. In our previous paper [14], for Raman spectra of DPP the accordion vibrational mode has provided evidence that preferential stabilization of a specific molecular form about the P–O bonds occurs even in the solid state, depending upon the content of hydrated water molecules about the PO_4^- group.

In the present study, the accordion vibrational modes, which reflect directly the conformation about the P–O bonds, has been measured for the micellar solution of the DPP-water system. The very broad Raman band at 270 cm^{-1}, which derives from the GT form [14], has been found (spectra not shown), indicating that the GT form about the P–O bonds is stabilized in the micellar state. However, the broadness of the 270 cm^{-1} band may indicate that other two molecular forms (GG and TT) also coexist in addition to the GT form, although their populations are low.

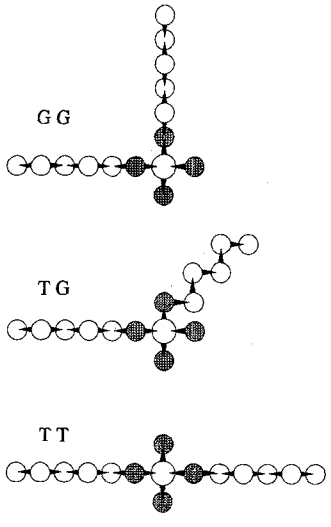

Fig. 6 Schematic representation of three rotational isomers (GG, GT and TT) about the P-O bonds. The conformations about every CH_2–CH_2 bond and two CH_2–O bonds were assumed to be in the trans conformation

Conclusion

For the DPP–D_2O solution, SANS spectra have been measured at various concentrations. In the SANS intensity spectra, very broad peaks were observed, indicating the presence of interactions between micelles. It has also been found that an interparticle structure factor is enhanced with an increase in micellar concentration.

The SANS intensity spectra have been analyzed, assuming mono- and poly-dispersity. The results analyzed on the basis of mono-dispersity are summarized as follows.

The aggregation number (**n**) for the DPP micelle depends on the concentration. All the **n** values fall on a straight line in the plot of $(X\text{-}X_{CMC})^{1/2}$ vs. **n**, showing that a ladder model of micellar growth can be applied to the micellar formation.

A minimum aggregation number ($\mathbf{n} = 7$) for a micelle at the CMC was assumed by extrapolation of the $(X\text{-}X_{CMC})^{1/2}$ vs. **n** plot. In the concentration range 7.0 ~ 10.0 wt%, the micellar shape is prolate and the **a**/**b** ratio depends on the concentration (**a**/**b** = 1.9 for 7.0 wt%, and **a**/**b** = 2.3 for 10.0 wt%). Furthermore, for the minimum micelle, an **a**/**b** ratio of 1.1 can be calculated, indicating that the minimum micelle may be spherical. For the DPP micellar system, we can assume that micellar growth and variation from the spherical to the prolate shape occur with an increase in concentration above the CMC.

Acknowledgement We express gratitude to Prof. Charmian J. O'Conner (University of Auckland, Department of Chemisty, New Zealand) and Dr. Tadashi Kato (Department of chemistry, Tokyo Metropolitan University, Japan) for reading the manuscript prior to publication and making suggestions for its revision.

References

1. Nakagaki M, Handa T (1975) Bull Chem Soc Jpn 48:630–635
2. Kunitake T, Okahata Y (1977) J Amer Chem Soc 99:3860–3861
3. Kunitake T, Okahata Y (1978) Bull Chem Soc Jpn 51:1877–1879
4. Kano K, Romero A, Djermouni B, Ache HJ, Fendler JH (1979) J Amer Chem Soc 101:4030–4037
5. Shimomura M, Kunitake T (1982) J Am Chem Soc 104: 1757–1759
6. Wagenaar A, Rupert LAM, Engberts JBFN, Hoekstra D (1989) J Org Chem 54:2638–2642
7. Sudholter EJR, Engberts JBFN, Hoekstra D (1980) J Amer Chem Soc 102:2467–2469
8. Sudholter EJR, de Grip WJ, Engberts JBFN (1982) J Amer Chem Soc 104:1069–1072
9. Rupert LAM, Hoekstra D, Engberts JBFN (1985) J Amer Chem Soc 107: 2628–2631
10. Rupert LAM, Van Breemen JFC, Van Bruggen EFJ, Engberts JBFN, Hoekstra D (1987) J Membr Biol 95:255–263
11. Rupert LAM, Hoekstra D, Engberts JBFN (1987) J Colloid Interface Sci 120:125–134
12. Shimanouchi T, Tsuboi M, Kyogoku Y (1964) Adv Chem Phys 7:435–498
13. Okabayashi H, Yoshida T, Ikeda T, Matsuura H, Kitagawa T (1982) J Amer Chem Soc 104:5399–5402
14. Okabayashi H, Taga K, Miyagai K, Uehara T, Yoshida T, Nishio E (1991) J Phys Chem 95:7932–7938
15. Okabayashi H, Okuyama M, Kitagawa T (1975) Bull Chem Soc Jpn 48:2264–2269
16. Okabayashi H, Taga K, Tsukamoto K, Tamaoki H, Yoshida T, Matsuura H (1985) Chemica Scripta 25:153–156
17. McCombie H, Saunders BC, Stacey GJ (1945) J Chem Soc, 380–382
18. Mukaiyama T, Fujisawa T (1961) Bull Chem Soc Jpn 34:812–813
19. Vass S, Török T, Jákli G, Berecz E (1989) J Phys Chem 93:6553–6559
20. Marcus YJ (1983) J Solution Chem 12:271–275
21. Suzuya K (1992) Ph D thesis, Tohoku University
22. Hirata H, Aoki S, Taga K, Okabayashi H, Yoshida T, to be published
23. Bendedoch D, Chen SH (1984) J Phys Chem 88:648–652
24. Tanford C (1972) J Phys Chem 76: 3020–3024
25. Hayter JB, Penfold J (1981) Mol Phys 42:109–118
26. Hansen J, Hayter JB (1982) Mol Phys 46:651–656
27. Kotlarchyk M, Chen SH (1983) J Phys Chem 79:2461–2469
28. Chen SH, Lin TL (1987) Method of Experimental Physics Vol 23, PART B, Chapt 16 Academic Press
29. Missel PJ, Mazer NA, Benedek GB, Young CY, Carrery MC (1980) J Phys Chem 84:1044–1057
30. Shew EY, Chen SH, Huang JS (1987) J Phys Chem 91:3306–3310
31. Burkitt SJ, Ottewill RH, Hayter JB, Ingram BT (1987) Colloid Polym Sci 256:619–627
32. Israelachvili J (1992) Intermolecular & Surface Forces, Chap 16 ~17 Academic Press
33. Kamo O, Matsushita K, Terada Y, Yoshida T, Okabayashi H (1984) Chem Scripta 23:189–194